Lactate Dehydrogenase Undergoes a Substantial Structural Change to Bind its Substrate

Linlin Qiu, Miriam Gulotta, and Robert Callender
Department of Biochemistry, Albert Einstein College of Medicine, Bronx, New York

ABSTRACT Employing temperature-jump relaxation spectroscopy, we investigate the kinetics and thermodynamics of the formation of a very early ternary binding intermediate formed when lactate dehydrogenase (LDH) binds a substrate mimic on its way to forming the productive LDH/NADH·substrate Michaelis complex. Temperature-jump scans show two distinct submillisecond processes are involved in the formation of this ternary binding intermediate, called the encounter complex here. The on-rate of the formation of the encounter complex from LDH/NADH with oxamate (a substrate mimic) is determined as a function of temperature and in the presence of small concentrations of a protein destabilizer (urea) and protein stabilizer (TMAO). It shows a strong temperature dependence with inverse Arrhenius behavior and a temperature-dependent enthalpy (heat capacity of 610 ± 84 cal/Mol K), is slowed in the presence of TMAO and speeded up in the presence of urea. These results suggest that LDH/NADH occupies a range of conformations, some competent to bind substrate (open structure; a minority population) and others noncompetent (closed), in fast equilibrium with each other in accord with a select fit model of binding. From the thermodynamic results, the two species differ in the rearrangement of low energy hydrogen bonds as would arise from changes in internal hydrogen bonding and/or increases in the solvation of the protein structure. The binding-competent species can bind ligand at or very near diffusion-limited speeds, suggesting that the binding pocket is substantially exposed to solvent in these species. This would be in contrast to the putative closed structure where the binding pocket resides deep within the protein interior.

INTRODUCTION

An enzyme balances two apparently conflicting requirements to function properly. In forming the so-called Michaelis complex, the bound substrate is positioned within the protein in close contact with key protein groups that facilitate catalysis. Additionally for bimolecular reactions, the two bound substrates are held tightly together and positioned correctly for chemical reaction. Generally, static pictures involving no motion of the reacting groups are used to yield working mechanistic pictures. On the other hand, a second requirement of enzymatic catalysis is effective substrate binding and, the reverse, product release. Substrate is captured from solution and shuttled in and out of the binding pocket of the active site in a timely manner, typically on the order of a millisecond. Binding is necessarily a dynamical process. Substantial motions within the protein complex are required, including the recruitment of key proteins groups into the active site and desolvation and closure of the binding pocket. This often involves the motion of an active site loop, wherein an open form can facilitate ligand binding and release, and a closed form prepares, controls, and protects the reacting species. The dynamics of ligand binding to proteins is little understood, but involve motions from femtoseconds to tens of milliseconds (and sometimes even longer), and the process for enzymes is such that the enzyme·substrate complex lives just long enough to permit effective catalysis and no longer. The goal of this work is to examine the dynamics of how the Michaelis complex is formed in lactate dehydrogenase (LDH). We focus on how the enzyme·ligand encounter complex is formed; the encounter-complex species is of special importance in understanding the binding process.

LDH catalyzes the direct transfer of a hydride ion from the *pro*-R face of the reduced nicotinamide group of NADH to the C_2 carbon of pyruvate producing NAD+ and the alcohol lactate, accelerating the solution chemical reaction by some 14 orders of magnitude (1). Binding of substrate to LDH is ordered and follows the formation of the LDH/NADH binary complex. The substrate binding pocket lies deep within the protein, buried ~10 Å from the protein's surface (2–4; see Fig. 1), although our recent molecular dynamic calculations suggest that the protein samples conformations wherein the binding pocket is substantially exposed to solvent (4). It supplies the catalytically crucial His^{195}, and the preformed pocket additionally solvates the substrate's charged carboxyl group by supplying Arg^{171} (5). The rate-limiting step in the turnover of LDH is not the chemical hydride transfer step but rather loop motion involving closure of the so-called mobile loop (surface residues 98–110), occurring in a time of ~1–10 ms (6,7).

Our previous studies (7,8) on the dynamics of forming the productive LDH/NADH·substrate Michaelis complex show that binding takes place via a sequence of steps: the formation of an encounter complex in a bi-molecular step followed by two unimolecular transformations on the microsecond/millisecond timescales. The various key components of the catalytically competent architecture are brought together as separate events with the formation of strong hydrogen bonding

Submitted March 22, 2007, and accepted for publication April 23, 2007.

Address reprint requests to Dr. Robert Callender, Tel.: 718-430-3024; E-mail: call@aecom.yu.edu.

Editor: Jonathan B. Chaires.

0006-3495/07/09/1677/10 $2.00

doi: 10.1529/biophysj.107.109397

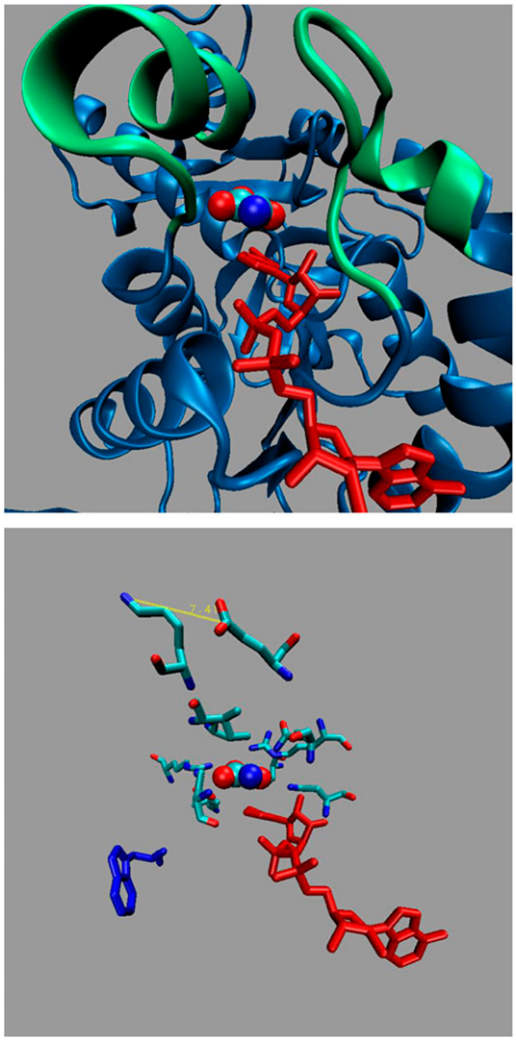

FIGURE 1 Two structural diagrams of LDH with NADH and oxamate bound. For both, oxamate is shown as space filling in standard colors. NADH is shown as a red stick figure. LDH is blue, with the exception of the loop region and the α-helix it binds to upon loop closure (*green*). (*Top*) Ligands are shown within the active site, with the active site 10 Å from the surface of the protein. (*Bottom*) The active site with the protein ribbon structure removed. Only protein residues within 5 Å of oxamate are shown. The affected tryptophan (*dark blue*) and the two residues that are responsible for loop closure (located in *green section* shown in *top panel*) are shown. The loop closed distance between these two residues is 7.4 Å (*yellow dashed line*). Structure from 1I0Z. For a space-filling view of the closed structure of LDH/NADH and picture of a putative open conformation, see Pineda et al. (4).

between active site His^{195} and substrate early in binding and the closure of the mobile loop, and movement of Arg^{109} located within the loop, over the bound substrate as the final event in the binding process.

Our studies of LDH have been quite detailed. Observation of submillisecond timescales is achieved by employing laser-induced temperature-jump (T-jump) relaxation spectroscopy, an approach that can provide resolution on the picosecond timescale (9–11). T-jump relaxation experiments monitor the return to equilibrium of a chemical system after a sudden increase in temperature, produced in our studies by absorption of pulsed laser light tuned to a weak near-infrared water band. Evolving structure has been probed using both transient NADH visible fluorescence emission and IR absorption spectroscopies; the latter provides specific information on the occurrence of key electrostatic interactions at the active site. We have studied the binding kinetics for the LDH/NADH binary complex with oxamate ($NH_2(C{=}O)COO-$), an excellent nonreactive substrate mimic (12,13). In this way, atomic motion associated with the binding pathway can be separated from that associated with chemical steps occurring during catalysis. For example, there is good reason to believe that the encounter complex is quite evolved toward the Michaelis complex. Although the key residues, His^{195}, Arg^{171}, and Arg^{109} are not yet in proper contact with bound substrate mimic (7), oxamate is almost certainly bound within the not-yet fully formed active site of the enzyme (8). Under suitable experimental conditions, the observed on-rate of LDH/NADH with oxamate to form the LDH/NADH·oxamate encounter complex is easily measured. This study examines the response of the observed on-rate to temperature and small concentrations of a destabilizer (urea) and stabilizer (TMAO) of protein structure (e.g., (14)). The kinetic and thermodynamic results are interpreted in terms of implied structural features required of LDH/NADH for efficient binding and have served as the experimental base for detailed theoretical calculations on this issue (4).

How proteins bind their ligands has long been a matter of intense interest. For enzymes, an early model proposed that the enzyme-binding pocket is preformed, complementary to substrate, and competent to bind substrate; this so-called lock-and-key picture has clear difficulties recognized now for quite some time (e.g., (15)). More recently, two views of the binding process have emerged. One states that the unligated protein exists in a single conformation, either binding-competent or not, and that interaction with the ligand induces conformational changes affecting both the protein and ligand leading to the proper structure of the bound state(s); this induced-fit model was developed to explain how a single enzyme could have substantially different catalytic competence for closely related ligands (16) and is, for example, the basis for the Koshland-Nemethy-Filmer model of allosteric regulation of proteins. Another model proposes that the unligated enzyme in solution is viewed as inherently dynamic and exists as an equilibrium of interconverting conformations, some competent to bind and others not. Effectively the ligand picks out a certain structural subset of the unligated protein in the preexisting equilibrium and binds to these; some recent literature has referred to this as selected fit. Such a mechanism is the basis for the Monod-Wyman-Changeux model of allosteric regulation. The preexisting equilibrium molecular model for binding appears also to be useful in understanding how proteins can adopt substantial functional diversity (e.g., 15).

MATERIALS AND METHODS

Materials

Pig heart H_4-L-lactate dehydrogenase (LDH) (10 mg/ml ammonium sulfate suspension), pyruvate (pyruvate monosodium salt) and NADH (s) are from Roche Scientific (Nutley, NJ); oxamic acid as sodium salt (s) from Acros Organics (Geel, Belgium), and mono- and di-basic sodium phosphate (s) from Fisher Scientific (Pittsburgh, PA).

LDH stock solution

Two-to-three milligrams of LDH (Roche) were dialyzed three times against 0.1 N sodium phosphate pH 7.2 buffer at 4°C. The dialyzed enzyme solutions were filtered through 0.45 μM filters. The concentration of LDH was determined by UV absorption using $A_{280} = 50\ mN^{-1}\ cm^{-1}$, where N is the normality of the enzyme solution, the concentration of identical binding sites. When higher concentration stocks were needed, model No. MWCO 1000 centricon or microcon concentrators (Millipore, Billerica, MA) were used.

Activity assay

The activity of the enzyme was determined through UV absorption by monitoring the reduction of NADH ($\varepsilon_{340} = 6.22\ mM^{-1}\ cm^{-1}$) to NAD^+ in the redox reaction with pyruvate being oxidized to lactate (17,18). Addition of LDH was used to start the assay reaction. Note that only stock solutions $<$24 h old with $A_{260}/A_{340} \leq 2.4$ were used. The UV spectrometer used was a model No. DU7400 (Beckman Coulter, Fullerton, CA).

Steady-state measurements

The CD spectrophotometer used was a model No. J-720 equipped with a thermostated cell holder (JASCO, Easton, MD). The fluorimeter used was a thermostated Fluoromax 2 (Spectra Physics, Mountain View, CA). Rectangular quartz cuvettes were used for both the temperature-monitored CD and fluorescence measurements. For the CD measurements, the cuvette pathlength was 2 mm. The fluorescence measurements used a 1-cm pathlength cuvette. For every sample spectrum run, a background spectrum was subtracted and the data was adjusted for dilution effects.

Due to the small but clear trends in the steady-state fluorescence measurements, we applied single value decomposition (SVD) analysis, a useful procedure for quantifying small trends (see e.g., (19)). SVD analysis is a means of expressing experimental data as a sum of orthogonal basis set vectors (eigenvectors). The amplitude of each vector (eigenvalue) determines the relative importance of each basis set vector in reproducing the data. Analysis is based on the SVD theorem, $X_{m\times n} = U_{m\times n} \cdot S_{n\times n} \cdot V^{T}_{n\times n}$, where $X_{m\times n}$ is a rectangular matrix of experimental data or parameters (fluorescence wavelength and intensity, in our case). U_{mxn} has the same dimensions as X, and its columns contain the L left singular vectors, $\{u_k\}$, which form the orthonormal basis set (eigenvectors). L is the rank of the matrix. $S_{n\times n}$ is a diagonal matrix of the amplitudes of the vectors in U required to reproduce the data curve. The data is ordered so that $s(1,1) > s(2,2) > \ldots\ldots\ldots > s(L,L)$. A plot of S is amplitude versus index. The earliest value will be very high, then the values will steeply decline until a break point is reached; these are the significant values. The method is important because fitting of the data usually involves inversion of the matrix equation; for example, in a linear least-squares fit. If the chosen basis set does not uniquely represent the data, then some of the values in the matrix S will be very small (in our case, after the break), and inversion results in a poorly behaved numerical fit. The values after the break point will decline much more slowly; and represent noise in the data. Thus, the method allows this noise to be ignored by zeroing the relevant components in the singular value matrix S. V^{T}_{nxn} is also an orthonormal $n\times n$ matrix. Its rows are the right singular vectors, $\{v_k\}$. An SVD plot of u_1 vs. wavelength is a fluorescence-versus-wavelength plot that shows the most relevant orthonormal component. We label λ_{scm} as the center-weighted wavelength, which is the maximum frequency of this plot.

T-jump samples

Binary mixtures of 80 μM:80 μM LDH:NADH in 0.1 M sodium phosphate buffer were incubated at 4°C for 30 min before the addition of oxamate (1200 μM) or osmolytes (TMAO or urea). The ternary sample was incubated at 4°C for 30 min before it was used. The samples were dialyzed through 0.2 μM filters right before they were loaded into 0.2-mm quartz cuvettes.

T-jump spectrometer

The temperature-jump fluorescence relaxation kinetic setup has been described previously (20). The heating beam uses light from a pulsed Nd/YAG laser (model No. GCR-150-10, Spectra Physics), operating at 1064 nm and Raman-shifted to 1541 nm. The beam is focused on the sample cell into a spot of ~1 mm diameter. In this configuration, the laser provides sufficient energy to produce a temperature jump in water of up to 20°C. The probe beam is provided by a CW Ar^+ ion laser (Coherent, Santa Clara, CA). A group of lines near 360 nm is used for NADH fluorescence excitation; power levels incident on the sample were set to cause minimal sample photodamage, typically 5–10 mW focused into a 300-μm diameter spot. Detection is by an off-axis PMT with emission wavelength selected by a bandpass filter (Coherent Model No. 35-5024, centered at 450 nm with a full width at half-maximum of 40 nm). Real-time determination of temperature in the excitation volume was done by measurement of light transmission at 1460 nm, the maximum of a water absorption band. The cuvette holder is water-jacketed with the temperature (the initial temperature of the sample before the jump) controlled by a water bath.

In every measurement cycle, the fluorescence excitation laser beam was opened 4 ms before the heating pulse and closed 15 ms after the pulse to prevent UV bleaching of the sample. Temperature of the heated volume returns to initial value after ~300 ms. The spectrometer is operated at 1 Hz, and the results of all measurements are averaged. The experiments described here typically required 1500–3000 individual measurements to obtain the desired S/N ratio. The kinetic data were digitized using two oscilloscopes: models No. TDS-754A and No. TDS-420 (Tektronix, Beaverton, OR).

RESULTS AND DISCUSSION

Kinetic studies

Previously, we determined the pathway for the binding of oxamate to LDH/NADH using a combination of stopped-flow and laser-induced temperature-jump approaches; the dynamic range of the combined approaches covered 10 ns to minutes, some 10 orders of magnitude. Evolving structure was monitored from modulations of the fluorescence emission of the reduced nicotinamide group of NADH (8) and from changes in the stretching frequencies of key bonds of oxamate, which were identified via isotope-edited infrared absorption spectroscopy (7). The following binding pathway was determined as

$$\mathrm{LDH/NADH} + \mathrm{oxamate} \underset{k_{off}}{\overset{k_{on}^{app}}{\rightleftarrows}} \mathrm{LDH^1/NADH \cdot oxamate} \underset{k_{2\to1}}{\overset{k_{1\to2}}{\rightleftarrows}} \mathrm{LDH^2/NADH \cdot oxamate} \underset{k_{3\to2}}{\overset{k_{2\to3}}{\rightleftarrows}} \mathrm{LDH^3/NADH \cdot oxamate} \quad \text{(Scheme I)}$$

where the species LDH[3]/NADH·oxamate is presumed to represent the active Michaelis complex. Here we will find that this kinetic pathway is incomplete.

In the present studies, we are interested in determining the rate constant, k_{on}^{app}, as a function of temperature and a variety of organic osmolyte conditions. The value of k_{on}^{app} is rather high but easily within the time resolution of laser-induced T-jump approaches. We are denoting here the on-rate constant as apparent, k_{on}^{app}, for reasons that will become clear below; in our previous studies, this rate constant was referred to as k_{on} (8).

In the T-jump relaxation studies, specific concentrations of LDH, NADH, and oxamate result in an equilibrium mixture of the various species in Scheme I. Equimolar amounts of LDH and NADH are first added together and the binary complex is formed during the equilibration period (see Materials and Methods). For the T-jump studies, the concentration of each is 80 μM, so that at equilibrium >90% of the LDH is bound with NADH, regardless of the temperature. The resulting LDH/NADH solution is then mixed with saturating amounts of oxamate (1200 μM). After the ternary sample has equilibrated, >97% of the LDH/NADH has now been incorporated into LDH/NADH·oxamate regardless of the equilibration temperature. After the rapid change in temperature, the chemical system relaxes to a new equilibrium, and its relaxation can be monitored by the changing emission from the NADH-reduced nicotinamide group. At high concentrations of oxamate, the fastest observed relaxation rate, k_{obs}, is assigned to the association/dissociation event (8), $k_{obs} = k_{on}^{app} \cdot ([\text{oxamate}]_{free} + [\text{LDH/NADH}]_{free}) + k_{off}$. The resulting T-jump scan for a typical aqueous ternary sample where LDH/NADH·oxamate is 80 μM:80 μM:1200 μM and T_f = 27.0°C is shown in Fig. 2. Double-exponential kinetics are observed; the major component of the relaxation kinetics is the association/dissociation event while the second event has been assigned to the unimolecular conversion of ternary complex species labeled 1 to species 2 in Scheme I above. This observed rate of the fastest event under our conditions, $k_{obs} = k_{on}^{app} \cdot [\text{oxamate}]_{free}$ since $[\text{oxamate}]_{free} \gg [\text{LDH/NADH}]_{free}$ and $k_{on}^{app} \cdot [\text{oxamate}]_{free}$, is ~20 times larger than k_{off}.

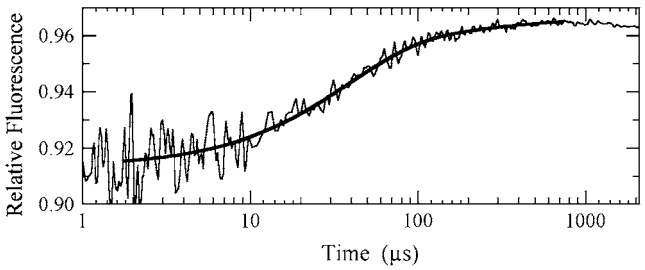

FIGURE 2 Time course of fluorescence emission at 450 nm (excitation 360 nm) of ternary complex LDH/NADH·oxamate 80:80:1200 μM in 0.1 M pH 7.2 sodium phosphate buffer in response to a laser-induced temperature jump, final temperature of 26.5°C. Double-exponential fit gives rates of 38.0 (major component) and 4.0 (minor component) ms^{-1}.

There is a signal in the relaxation studies arising from the LDH + NADH to LDH/NADH side reaction since the change of concentration of these species, despite being very small, is comparable to the change in concentration of the ternary complex species, LDH/NADH·oxamate, under our conditions; moreover, the emission from NADH is modulated when it binds to LDH in addition to when it combines with LDH/oxamate. We do expect, however, that the association/dissociation rate of the LDH/NADH complex will be very slow compared to the formation of the LDH/NADH·oxamate complex since the concentration of oxamate is very high in our solutions compared to LDH and NADH. We have previously examined the binding of NADH to LDH and have determined the bimolecular on- and off-rate constants for the reaction (20); simulations of the kinetics using the previously determined rate constants show that the binding reaction to form the binary complex occurs on the millisecond timescale, two orders-of-magnitude slower than the rates for the association/dissociation of the encounter complex of the ternary species observed under our experimental conditions. Hence, the side reaction does not complicate the analysis here.

Fig. 3 shows plots of normalized $\ln(k_{obs}(T)/k_{obs}(T_{ref}))$ versus $1/T$ in Kelvin in the temperature range of 20–52°C for ternary complexes LDH/NADH·oxamate 80:80:1200 μM in 0.1 M sodium phosphate pH 7.2 alone (Fig. 3 *B*), in the presence of 1 M TMAO (Fig. 3 *A*), and in the presence of 0.25 M urea (Fig. 3 *C*). The observed rate is proportional to the concentration of free oxamate, $k_{obs} = k_{on}^{app} \cdot [\text{oxamate}]_{free}$. Plotting the log of the normalized rate rids the function of the oxamate concentration and also permits more accurate fits to thermodynamic functions. There is notable curvature seen in the plot, as we have reported previously for the ternary complex in aqueous solution over a reduced temperature range (8). Here we also see that the osmolytes affect the degree of curvature with 0.25 M urea > aqueous > 1 M TMAO. The present results, over an extended temperature range relative to our previous study, show that the van 't Hoff enthalpy, describing k_{obs}, switches from being negative to positive; hence, the enthalpy associated with k_{obs} is temperature-dependent. Defining k_{obs} by the function exp-($\Delta G/RT$) where the Gibbs free energy includes a nonnegligible contribution from a heat capacity term (21) of $\Delta G = \Delta H - T\Delta S + \Delta C_p((T - T_{ref}) - T\ln(T/T_{ref}))$, the normalized observed rate reduces to

$$\ln\left(\frac{k_{obs}(T)}{k_{obs}(T_{ref})}\right) = \left(\frac{-1}{R}\right) \times \left(\Delta H \times \left(\frac{1}{T} - \frac{1}{T_{ref}}\right) + \Delta C_p \times \left(\left(1 - \frac{T_{ref}}{T}\right) + \ln\left(\frac{T_{ref}}{T}\right)\right)\right).$$

Fits to this function yields $\Delta H = -7.6 \pm 0.8$ kcal/M, $\Delta C_p = 610$ (± 84) cal/Mol K for the ternary system in aqueous solution at $T_{ref} = 298$ K (25°C). Our previous result, based on separate measurements over a limited temperature range, 17–37°C, yielded a heat capacity term of $\Delta C_p = 790 \pm 116$

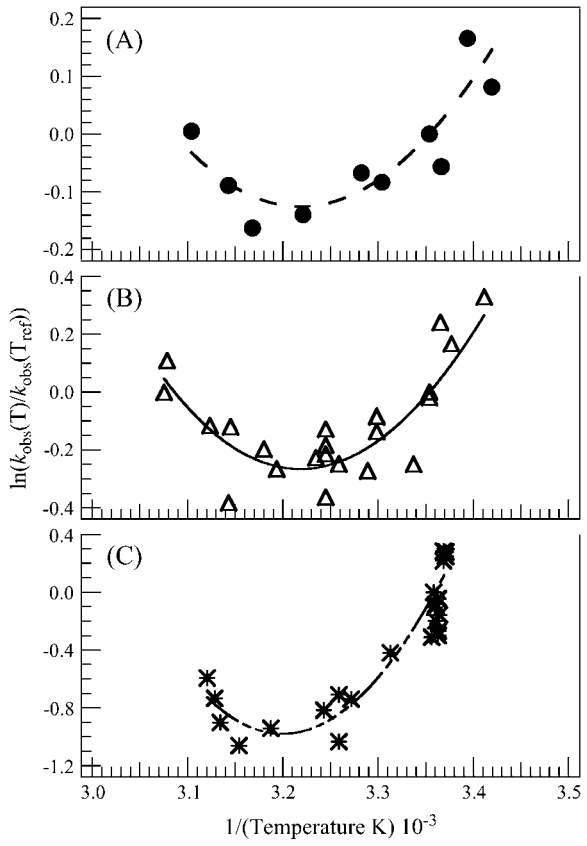

FIGURE 3 Plots of the observed relaxation rate showing the temperature dependence as $\ln(k_{obs}(T)/k_{obs}(T_{ref}))$ vs. $1/T$ (K) for ternary complexes LDH/NADH/oxamate 80:80:1200 μM in pH 7.2 sodium phosphate buffer alone (B), with 1 M TMAO (A), or with 0.25 M urea (C). $T_{ref} = 25°C$. Note that the relative range of y axes in panels A–C go in proportion as 1:2:4. The three panels illustrate osmolyte effects. The smooth lines are fits to a thermodynamic function, as described in the text.

cal/Mol K (8), in very good agreement with the present study. $\Delta H = -3.6 \pm 0.8$ kcal/M, $\Delta C_p = 288 \pm 80$ cal/Mol K for the ternary system in 1 M TMAO; and $\Delta H = -24 \pm 3$ kcal/M, $\Delta C_p = 1600 \pm 300$ cal/Mol K for the ternary system in 0.25 M urea.

The thermodynamic results can be understood as resulting from oxamate binding to a subset of the LDH/NADH microstates that are competent to bind the ligand. In fact, previous studies have suggested that lactate dehydrogenase complexed with NADH exists as an equilibrium of binding-competent/binding-noncompetent conformations (22). The anomalous temperature dependence associated for k_{obs} then results from the temperature modulation of the population of the binding-competent microstates. The high value of the heat capacity term is consequently understood as due to a substantial change in solvation character between competent and noncompetent LDH/NADH microstates (21,23). Processes causing changes in solvation character include exposure of hydrophobic residues to water. Assuming that the dominant contribution to the value of the heat capacity is exposure of hydrophobic moieties to solvation, we calculated the exposed surface area from empirical studies relating a change in accessible surface area (ASA) during the structural transition to ΔC_p ($\Delta C_p = -251 + 0.19(\Delta ASA)$; 24). We have $\Delta ASA = 4500$ (± 500) Å^2 for the measured heat capacity in aqueous solution (Fig. 3 B) determined above, $\Delta C_p = 610$ (± 84) cal/Mol K. Using the same empirical relationship between ΔC_p and ΔASA for the urea and TMAO solutions yields a ΔASA of 9700 (± 1500) Å^2 (0.25 urea), 4500 (± 500) Å^2 (buffer alone), and 2800 (± 400) Å^2 (1 M TMAO). Using the empirical relationship relating the number of residues exposed to solvent to accessible surface area established previously ($\Delta ASA = -907 + 93$ (number of residues); (24)), we calculate that for the complex in aqueous solution that 58 (± 6) residues are exposed to solvent. This is a large part of the 338-residue protein. We have performed recent molecular dynamics calculations to explore the conformational space accessible to LDH/NADH (4). The results of these calculations show that LDH/NADH can find structures that appear to be capable of binding ligand efficiently, where the active site is exposed to solvent and is considerably more open than others. High specific heats between open and closed conformations arise from subtle rearrangements in internal hydrogen bonding and an increased solvation of the protein structure (see Discussion).

Such findings, in any case, are consistent with the results above suggesting that urea opens up the LDH/NADH structure for binding of ligand while TMAO makes the structure of the binary complex more rigid or tight, less able to bind ligand. Such behavior is consistent with the known affects of these osmolytes on protein structure. This is directly probed in studies described below.

Assuming there are multiple LDH/NADH microstates, some competent to bind ligand and some not, a more complete kinetic model of the first step in the binding of substrate is (C = competent; NC = noncompetent):

$$\mathrm{LDH^{NC}/NADH} \underset{k_{C\to NC}}{\overset{k_{NC\to C}}{\rightleftarrows}} \mathrm{LDH^{C}/NADH} + \mathrm{oxamate} \underset{k_{off}}{\overset{k_{on}}{\rightleftarrows}} \mathrm{LDH^{1}/NADH \cdot oxamate} \rightleftarrows \ldots\ldots\ldots \qquad \text{(Scheme II)}$$

Assuming the first step is fast (see below) compared to the second ($k_{NC\to C} + k_{C\to NC} \gg k_{on}[ox], k_{off}$), the T-jump observed rates are given by

$$k_{obs}^{binary} = k_{NC\to C} + k_{C\to NC}$$

$$k_{obs} = \frac{k_{on}([LDH^C/NADH] + [ox])k_{NC\to C}}{k_{NC\to C} + k_{C\to NC}} + k_{off}.$$

There is reason to believe that the equilibrium between competent/noncompetent LDH/NADH species favors the noncompetent population (see below) so that $k_{C\to NC} > k_{NC\to C}$. In that case, and defining $K = k_{NC\to C}/k_{C\to NC}$, we have that

$$k_{obs} = \frac{k_{on}([LDH^C/NADH] + [ox])k_{NC\to C}}{k_{NC\to C} + k_{C\to NC}} + k_{off} \cong k_{on}K[ox],$$

so that the apparent rate constant determined in our study is $k_{on}^{app} = k_{on}K$. The strong temperature dependence of k_{on}^{app} arises from the temperature modulation of either the k_{on} term or the equilibrium constant, K, between competent and noncompetent LDH/NADH species. It is more likely that the temperature dependence mainly arises from the temperature dependence of K rather than the k_{on} term since k_{on} is very close to the diffusion rate-limited value; $k_{on}K = 2.0\ (\pm 1)\ 10^7\ M^{-1}\ s^{-1}$ at 35°C (8) with the value of K bracketed. Given an approximate upper limit of $10^9\ M^{-1}\ s^{-1}$ for diffusional encounters, $K > 0.01$; on the other hand, discussed below, there is evidence that the population of competent-binding LDH/NADH substates is smaller that that of noncompetent so that $K < 1.0$.

The interconversion between competent/noncompetent LDH/NADH species is not observed directly in our studies. All events observed in previous kinetic studies of the LDH/NADH + oxamate system involve oxamate (7,8), and so cannot arise from LDH/NADH interconversions, which would not involve oxamate. Studies ((20); and unpublished data) of the relaxation kinetics of LDH/NADH reveal events on multiple timescales from nanoseconds to microseconds, but none of these signals have the correct temperature dependence implied by the data of Fig. 3. We believe this is because the relative population of the competent species is small; as such, the signal of this relaxation event would be small. In our analysis, we have taken that the interconversion between competent and noncompetent conformers of LDH/NADH occurs on fast timescales for the following reasons. Whereas it has been known for some time that some enzymes do exist as two slowly interconverting conformers that bind ligand differently (e.g., (25); hysteretic enzymes), this behavior is observed in kinetic measurements of the catalytic behavior of the enzyme. None of this type of behavior has been detected in LDH, despite extensive studies. Moreover, if the process was very slow, all the thermodynamics would involve just k_{on}, and this is physically unreasonable. If the interconversions occurred on timescales similar to those observed in Scheme I, mixing of time constants would likely occur, and no mixing has been observed. Fast interconversions ($<10\ \mu s$) of the binary complex are observed in experiments (20), and calculations (4; see Discussion) suggesting that structural changes can take place of the type characterized here on very fast timescales.

The notion that the oxamate binds to a subset of LDH/NADH substates can be further probed by modulating the relative population of the substates by means other than temperature. Specifically, the relative populations of the microstates can be perturbed by osmolytes: the addition of a small amount of urea to the protein solution can be expected to open up the structure favoring the binding competent while trimethylamine-*n*-oxide (TMAO) closes down protein structure reducing peptide backbone exposure to solvent, thus favoring the binding-incompetent species (22,26). Such effects are perhaps most deeply probed by hydrogen-deuterion exchange studies of folded proteins (e.g., (14)).

Fig. 4 plots $k_{obs} = k_{on}^{app} \cdot [oxamate]_{free}$ as a function of the denaturant urea and structure protecting TMAO concentrations. As can be observed, the rate is modulated just as expected through the equilibrium constant term K in $k_{on}^{app} = k_{on}K$. We observed the increasing of binding rate with urea concentration up to 0.5 M. Further addition of urea causes the rate to decrease which is almost certainly due to the urea-caused dissociation of NADH from LDH/NADH as demonstrated in separate equilibrium binding measurement (data not shown). In contrast, TMAO causes a monotonically decreasing rate until the concentration reaches 0.8 M, beyond which the rate stays constant. Generally it is a good approximation to describe the Gibbs free energy between two protein forms, here between competent and noncompetent LDH/NADH microstates $\Delta G^{C\text{-}NC}$, as a linear function of the osmolyte concentration (21). Letting $\Delta G^{C\text{-}NC} = \Delta G^{C\text{-}NC}_{water} - m[\text{osmolyte}]$ and $K = \exp(-\Delta G^{C\text{-}NC}/RT)$, we find that $m_{urea} = 660\ (\pm 100)$ cal/mol M while $m_{TMAO} = -560\ (\pm 70)$ cal/mol M. We can calculate the ASA from urea determined *m*-values, $m = 374 + 0.11(\Delta ASA)$ (24); this yields a $\Delta ASA = 2600\ (\pm 900)$ Å, which is comparable to the ΔASA obtained

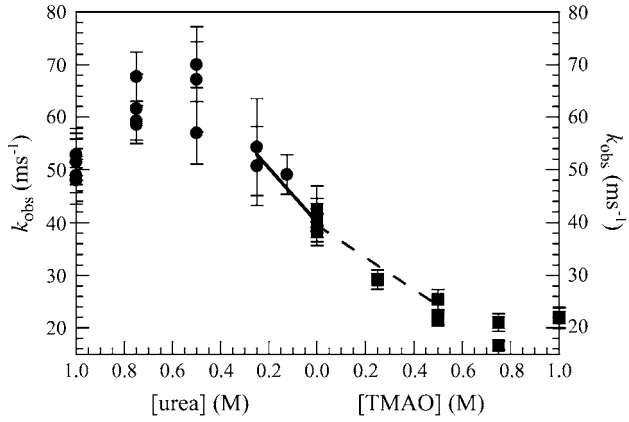

FIGURE 4 Observed reaction rate associated with the formation of the LDH/NADH·oxamate encounter complex, described as k_{obs} in the text, versus [urea] (●, *left*) and [TMAO] (■, *right*) for binary complex LDH:NADH 80:80 μM in 0.1 M sodium phosphate buffer, pH 7.2, at 25°C. Linear regions used for the *m*-value fits are (– – –) TMAO, and (——) urea. Calculated *m*-values for TMAO and urea are −560 (±70) and 660 (±100) cal/mol M, respectively.

from the heat capacity results above. That the ΔASA values obtained from two different thermodynamic measurements (variations with temperature and variations with a denaturant) are similar to each other is taken as strong evidence for the structural analysis presented herein.

TMAO is generally a stronger agent than is urea; its effective (absolute size) *m*-value magnitude is ~3:2 that of urea's (27). That the observed rate saturates at low values of [TMAO] and that the measured *m*-value for TMAO is comparable to urea both suggest that the binding-competent species is in the minority. Therefore, the addition of more TMAO would have a smaller and smaller proportional effect on the population of the minority species.

Structural studies

We performed numerous folding/unfolding studies of the LDH/NADH binary complex in an attempt to characterize any structural difference in binding-competent/noncompetent species. In general, we found evidence that LDH/NADH exists in multiple conformations whose relative populations are modulated by small changes in either temperature or osmolyte (urea). However, we were unable to discern any species directly related to the binding-competent species; this would be expected if the binding-competent species is a small minority, as suggested by the results presented above.

Several studies examined the amide-I IR band of the binary complex as a function of temperature. The protein's amide-I band is sensitive to solvation of both helices as well as sheet secondary structure. However, we observed no temperature-dependent changes in the LDH/NADH IR spectrum that correlate with the temperature dependence of the observed rate (Fig. 3) (data not shown).

Fig. 5 shows the CD spectrum of LDH/NADH at 222 nm, a wavelength particularly sensitive to changes in protein helical structure, as a function of urea concentration. The variation is quite unlike many proteins, which show a sharp cooperative melting transition, typically occurring at high (4–6 M) urea. Rather, the melting profile for LDH/NADH is fairly complicated: gradual changes indicating decreasing helical structure with [urea] at low urea (0–1 M), larger but still gradual changes from 1 to 2.3 M urea, and still further decrease in the (absolute) CD spectrum for still larger [urea]. The results show clearly that the structure of LDH/NADH is not cooperative, but rather the protein melts differently in different domains. Such behavior has been reported previously for LDH in substantial detail (28). Of particular interest in the context of the current studies is that, even at low urea concentrations (0–1 M), there is a clear effect on the structure of LDH/NADH; a small change in helical structure is uniformly observed over the entire region. This is consistent with, but certainly not proof of, a modulation of the relative populations of binding-competent/noncompetent species, one species having a different overall amount of helices.

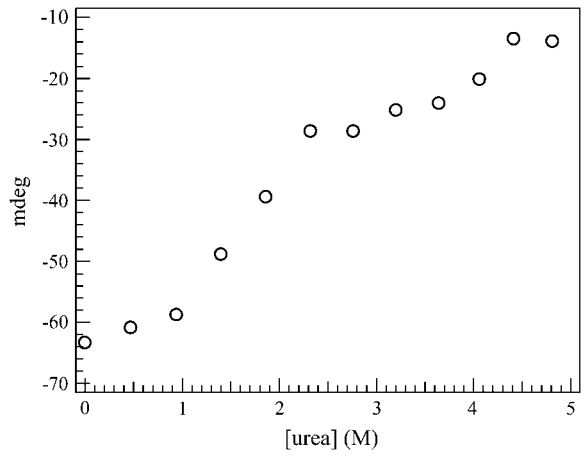

FIGURE 5 CD intensity (mdeg) at 222 nm for a sample of binary LDH/NADH 20:20 μM in 0.1 M sodium phosphate buffer pH 7.2.; a rectangular cuvette with a 2-mm pathlength was used. The buffer background was subtracted.

Fig. 6 shows melting of the LDH/NADH binary complex as a function to temperature using two measures of protein structure, CD at 222 nm and the λ_{max} value of highest magnitude SVD component (see Materials and Methods), the center-weighted wavelength (λ_{scm}), for each LDH/NADH Trp emission spectrum ($\lambda_{ex} = 290$ nm). The value λ_{scm} is more informative, but similar to λ_{max}. The λ_{scm} value pertains only to the highest signal component in the fluorescence spectrum; it is devoid of any noise effects. CD at 222 nm is a measure of overall helical content averaged over all the LDH/NADH species; Trp emission properties are often taken as an indication of local tertiary structure surrounding the emitting tryptophans. As monitored by CD at 222 nm (*solid circles*, *left axis*), the protein undergoes a cooperative

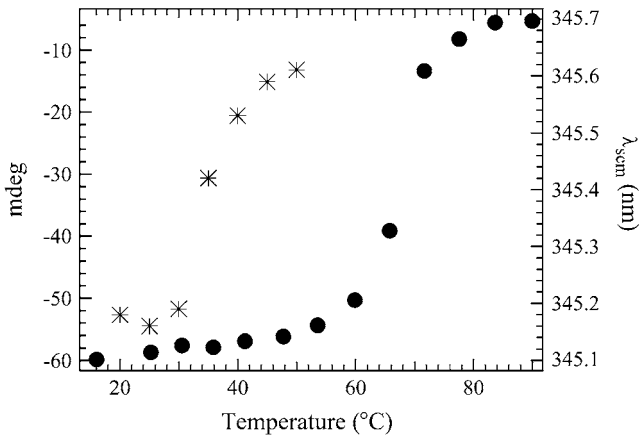

FIGURE 6 Temperature dependence for binary LDH/NADH measured by two different probes: ●, CD intensity in mdeg (*left axis*; 20:20 μM concentration loaded into a 2-mm rectangular cuvette with buffer background subtracted) and ✳, the center-weighted wavelength from each fluorescence spectrum (*right axis*; 4:4 μM concentration, sample loaded into a 1-cm rectangular cuvette). The sample was prepared in 0.1 M sodium phosphate buffer, pH 7.2.

melting transition near 70°C. This is in basic agreement with differential scanning calorimetry observations on the melting of rabbit muscle LDH (29). Again, the CD signal does not show any measurable changes above and below the transition temperature of 37°C indicated by the kinetic results above (Fig. 3). The right axis to Fig. 6 (*stars* in the diagram) shows the temperature dependence of λ_{scm}. There are seven Trp residues in pig heart LDH/NADH so that these studies are not able to yield any structural monitor local to any specific Trp residue. Unlike the CD melting results, the fluorescence results indicate that there is a small signal indicating a structural change at ~37°C, certainly showing that some (perhaps small) structural change occurs at the temperature where the temperature variation of k_{obs} is a minimum (Fig. 3). As above, the Trp emission data is consistent with, but certainly not proof of, a modulation of the relative populations of binding competent/noncompetent species, one species having a different fluorescence profile compared to the other.

DISCUSSION

In previous work, we showed that the substrate surrogate oxamate binds to LDH/NADH via the formation of a LDH/NADH·oxamate encounter complex; formation of the competent Michaelis complex occurs subsequently via two unimolecular isomerizations of the ternary complex (6–8,13). In this work, we have detailed how the on-rate describing the binding of oxamate by LDH/NADH to form the encounter complex responds to temperature and the osmolytes, urea and TMAO. Our interest is to inquire about what is required, on a molecular scale, to bring about the earliest event of the ligand binding pathway, the formation of the encounter complex. By examining the effective on-rate of ligand with LDH/NADH, conclusions are made about the earliest stages of binding.

The kinetic and structural conclusions from Results are as follows. An undoubtedly simplified but adequate kinetic model for the formation of the encounter complex is

$$\mathrm{LDH^{NC}/NADH} \underset{k_{C\to NC}}{\overset{k_{NC\to C}}{\rightleftarrows}} \mathrm{LDH^{C}/NADH} + \mathrm{oxamate} \underset{k_{off}}{\overset{k_{on}}{\rightleftarrows}} \mathrm{LDH^{EC}/NADH \cdot oxamate} \rightleftarrows \ldots\ldots$$

with EC denoting the encounter complex. The binary LDH/NADH binary system does not exist as a single conformation but rather exists as an ensemble of conformations. Some of the structures can competently bind substrate (represented by LDH^{C}/NADH). However, a majority of them either cannot bind substrate or else bind substrate very poorly (represented by LDH^{NC}/NADH). Those that are binding-competent appear to bind substrate at near-diffusion-limited speed since the observed apparent on-rate, given by $K \cdot k_{on}$ ($K = k_{NC\to C}/k_{C\to NC}$), is not far from the limits set by simple diffusion at 107 M^{-1} s^{-1}. With [LDH^{C}/NADH] < [LDH^{NC}/NADH] ($K < 1$; see Results), k_{on} approaches the diffusion-limited value of $\sim 10^{9}$ M^{-1} s^{-1}. Although we were unable to directly measure the rate of interconversion between binding-competent/noncompetent forms, it appears to be fast—on the 10–100 μs timescale, or faster.

The equilibrium between binding-competent/noncompetent forms, K, responds to temperature as well as destabilizing (urea) and stabilizing (TMAO) osmolytes. The response to the osmolytes is just like that observed in hydrogen/deuterion exchange studies where the protein is in equilibrium between closed-to-solvent (nonexchangeable) and open-to-solvent (exchangeable) conformations (e.g., (14)). The response pattern to both temperature and osmolytes is the same as that found for proteins undergoing a structural transition between two conformations that involves changes in a substantial number of low energy bonds (bonds made and broken). We have indicated these simply as open (binding competent) and closed (noncompetent) conformations. We have previously speculated (8) that this transition involves either the exposure of hydrophobic groups to solvent or the changing of the hydrogen-bonding patterns of water molecules (when, for example, structural waters of the protein move to solvent). However, our recent calculations (4) suggest that the structural change may be more subtle, involving subtle protein and water rearrangements (see below).

The results of our study are in accord with the select-fit model of binding in that the substrate analog, oxamate, binds to only a portion of a preexisting equilibrium mixture LDH/NADH conformations in forming the encounter complex. However, it is not clear whether or not the binding-competent LDH/NADH conformations also respond structurally to the presence of the ligand in forming the encounter complex. Moreover, once the encounter complex is formed, our previous results show that the protein structure responds in such a way that the ligand makes key binding patterns and forms a catalytically competent ternary LDH/NADH·substrate conformation. Key binding patterns include the formation of key H-bonds between the substrate's C=O group with His^{195} and Arg^{109} as well as the salt bridge between the substrate's −COO− moiety and Arg^{171}. These later transformations are in accord with an induced-fit model of binding. We suspect that in general, both the select-fit and induced-fit mechanisms play a role in the binding of ligands to proteins as our current results indicate that they do for lactate dehydrogenase.

Why would nature choose to have proteins go about binding via a minority population of binding-competent species?

This seems inefficient. There are, however, several reasons why this is advantageous. One is that proteins, being finite in size and held together in their folded structures by low energy bonds, are inherently dynamical. Although static structural pictures of proteins invariably show us a single structure, it has long been appreciated that proteins sample a variety of conformations on a variety of timescales. The observation of trace populations is especially difficult; however, protein structures that are very different from the majority population yet differ by just a small energy difference (a few times *RT* or less) can well exist, given that the stability of a folded protein is only 5–15 kcal/mol (compared to $RT = 0.6$ kcal/mol at room temperature). It is well established that even small proteins can contain domains that are very labile to substantial unfolding. LDH has been shown to contain domains of very limited stability (28).

Another reason is that this method of binding may well be very efficient in getting the job done. The active site of LDH is buried, being 10 Å from the protein's surface. If the ligand's pathway from the surface to the interior is rigid, the process of getting into the active site pocket could be very difficult. On the other hand, if the structure of even a minority of the protein population is loosened or opened so that the binding pocket is accessible to solvent and the ligand can find its way to the vicinity of the pocket at diffusion limited speeds, the overall effect of this, if the proper balance is achieved, can be a binding rate sufficient for catalysis. Binding rates and the overall binding constants need only fulfill the requirements of efficient metabolism. In terms of rate, enzymatic catalysis typically occurs on the millisecond timescale (30), which is the time it takes small molecules to diffuse across cellular dimensions. In terms of binding constants, the K_m values of enzymes are typically approximately set to substrate cellular concentrations, thus yielding an enzyme half-full/half-empty in the cellular environment. The process of a transient change in structure that exposes a protein binding pocket to ligand has been supposed for some time. The classic example is that of the binding of oxygen to myoglobin. The binding pocket is so buried within the protein's quite hydrophobic interior that it seems impossible for the ligand to penetrate to the binding site without dynamic fluctuations of some sort.

We recently performed molecular dynamics calculations to explore the conformational degrees of freedom accessible to the LDH/NADH binary complex and to explore what structural factors can give rise to the substantial heat capacity observed in experiments (4). We found that LDH/NADH samples a wide range of protein conformations, some of which offer rather facile access of solvent to the active site. These open conformations do not require large-scale unfolding/melting of the binary complex. Rather, open versus closed conformations are due to subtle protein and water rearrangements which are, however, quite sufficient to explain the rather high value of heat capacity difference found for the two structure(s). The results suggest that the mobile loop of LDH is perhaps just partially open in the open conformations, with Arg^{109} positioned very well to interact electrostatically with incoming substrate and guide it to the active site. We also found that multiple open conformations, yielding multiple binding pathways, are likely.

This work was supported by the Institute of General Medicine of the National Institutes of Health, program project grant No. 5P01GM068036 and by National Institute of Biomedical Imaging and Bioengineering grant No. EB001958.

REFERENCES

1. Burgner, J. W., and W. J. Ray. 1984. On the origin of lactate dehydrogenase induced rate effect. *Biochemistry.* 23:3636–3648.
2. Holbrook, J. J., A. Liljas, S. J. Steindel, and M. G. Rossmann. 1975. Lactate dehydrogenase. *In* The Enzymes, 3rd Ed. P. D. Boyer, editor. Academic Press, New York.
3. Griffith, J. P., and M. G. Rossmann. 1987. M4 Lactate Dehydrogenase Ternary Complex with NAD and Oxamate. Brookhaven Data Bank 1LDM.
4. Pineda, J. R. E. T., R. Callender, and S. D. Schwartz. 2007. Ligand binding and protein dynamics in lactate dehydrogenase. *Biophys. J.* 93:1474–1483.
5. Deng, H., J. Zheng, A. Clarke, J. J. Holbrook, R. Callender, and J. W. Burgner. 1994. Source of catalysis in the lactate dehydrogenase system: ground state interactions in the enzyme·substrate complex. *Biochemistry.* 33:2297–2305.
6. Dunn, C. R., H. M. Wilks, D. J. Halsall, T. Atkinson, A. R. Clarke, H. Muirhead, and J. J. Holbrook. 1991. Design and synthesis of new enzymes based upon the lactate dehydrogenase framework. *Phil. Trans. Roy. Soc. (Lond.) B.* 332:177–185.
7. McClendon, S., D. Vu, R. Callender, and R. B. Dyer. 2005. Structural transformations in the dynamics of Michaelis complex formation in lactate dehydrogenase. *Biophys. J.* 89:L7–L9.
8. McClendon, S., N. Zhadin, and R. Callender. 2005. The approach to the Michaelis complex in lactate dehydrogenase: the substrate binding pathway. *Biophys. J.* 89:2024–2032.
9. Cantor, C. R., and P. R. Schimmel. 1980. Biophysical Chemistry. W. H. Freeman, San Francisco, CA.
10. Callender, R., and R. B. Dyer. 2002. Probing protein dynamics using temperature jump relaxation spectroscopy. *Curr. Opin. Struct. Biol.* 12: 628–633.
11. Dyer, R., F. Gai, W. Woodruff, R. Gilmanshin, and R. Callender. 1998. Infrared studies of fast events in protein folding. *Accts. Chem. Res.* 31: 709–716.
12. Parker, D. M., D. Jeckel, and J. J. Holbrook. 1982. Slow structural changes shown by the 3-nitrotyrosine-237 residue in pig heart[$Try(3NO_2)^{237}$] lactate dehydrogenase. *Biochem. J.* 201:465–471.
13. Clarke, A. R., A. D. B. Waldman, K. W. Hart, and J. J. Holbrook. 1985. The rates of defined changes in protein structure during the catalytic cycle of lactate dehydrogenase. *Biochim. Biophys. Acta.* 829:397–407.
14. Qu, Y., and D. W. Bolen. 2003. Hydrogen exchange kinetics of RNase A and the urea·TMAO paradigm. *Biochemistry.* 42:5837–5849.
15. James, L. C., and D. S. Tawfik. 2003. Conformational diversity and protein evolution—a 60-year-old hypothesis revisited. *Trends Biochem. Sci.* 28:361–368.
16. Koshland, D. E. 1958. Application of a theory of enzyme specificity to protein synthesis. *Proc. Natl. Acad. Sci. USA.* 44:98–104.
17. Burgner, J. W., and W. J. Ray. 1978. Mechanistic study of the addition of pyruvate to NAD catalyzed by lactate dehydrogenase. *Biochemistry.* 17:1654–1661.
18. Schmid, F., H.-J. Hinz, and R. Jaenicke. 1976. Thermodynamic study of binary and ternary complexes of pig heart lactate dehydrogenase. *Biochemistry.* 15:3052–3059.

19. Alter, O., P. O. Brown, and D. Botstein. 2000. Singular value decomposition for genome-wide expression data processing and modeling. *Proc. Natl. Acad. Sci. USA.* 97:10101–10106.

20. Deng, H., N. Zhadin, and R. Callender. 2001. The dynamics of protein ligand binding on multiple time scales: NADH binding to lactate dehydrogenase. *Biochemistry.* 40:3767–3773.

21. Fersht, A. 1999. Structure and Mechanism in Protein Science: A Guide to Enzyme Catalysis and Protein Folding. Freeman, New York.

22. Baskakov, L. V., A. Wang, and D. W. Bolen. 1998. Trimethylamine-*n*-oxide counteracts urea effects on rabbit muscle lactate dehydrogenase function: a test of the counteraction hypothesis. *Biophys. J.* 74:2666–2673.

23. Cooper, A. 2005. Heat capacity effects in protein folding and ligand binding: a re-evaluation of the role of water in biomolecule's thermodynamics. *Biophys. Chem.* 115:89–97.

24. Myers, J. K., C. N. Pace, and J. M. Scholtz. 1995. Denaturant *m*-values and heat capacity changes: relation to changes in accessible surface area of protein folding. *Protein Sci.* 4:2138–2148.

25. Frieden, C. 1979. Slow transitions and hysteric behavior in enzymes. *Annu. Rev. Biochem.* 48:471–498.

26. Hochachka, P. W., and G. N. Somero. 2002. Water-solute adaptations. *In* Biochemical Adaptation, Chapt. 6. Oxford University Press, Oxford.

27. Auton, M., and D. W. Bolen. 2005. Predicting the energetics of osmolyte-induced protein folding/unfolding. *Proc. Natl. Acad. Sci. USA.* 102:15065–15068.

28. Smith, C. J., A. R. Clarke, W. N. Chia, L. Irons, T. Atkinson, and J. J. Holbrook. 1991. Detection and characterization of intermediates in the folding of large proteins by the use of genetically inserted tryptophan probes. *Biochemistry.* 30:1028–1036.

29. Jacobson, A. L., and H. Braun. 1977. Differential scanning calorimetry of the thermal denaturation of lactate dehydrogenase. *Biochim. Biophys. Acta.* 493:142–153.

30. Radzicka, A., and R. Wolfenden. 1995. A proficient enzyme. *Science.* 267:90–93.